Elecrical Engineering (2007) 89:205–220
DOI 10.1007/s00202-005-0339-6

ORIGINAL PAPER

Guillermo A. Jiménez · Alfredo O. Muñoz
Manuel A. Duarte-Mermoud

Fault detection in induction motors using Hilbert and Wavelet transforms

Received: 1 June 2005 / Accepted: 4 November 2005 / Published online: 24 February 2006

Abstract In this work, a new on-line method for detecting incipient failures in electrical motors is proposed. The method is based on monitoring certain statistical parameters estimated from the analysis of the steady state stator current (for broken bars, saturation, eccentricities, and bearing failures) or the axial flux signal (for coil short-circuits in the stator windings). The approach is based on the extraction of the envelop of the signal by Hilbert transformation, pre-multiplied by a Tukey window to avoid transient distortion. Then a wavelet analysis (multi-resolution analysis) is performed, which makes the fault diagnosis easier. Finally, based on a statistical analysis, the failure thresholds are determined. Thus, by monitoring the mean value estimate it is possible to detect an incipient failure condition on the machine.

Keywords Hilbert transform · Wavelet transform · Fault detection · Broken bar detection · Motor fault detection · Motor failure diagnosis · Statistical analysis

1 Introduction

The first methods utilized to detect motor failures, such as chromatographic analysis, noise analysis, temperature analysis and vibration analysis, have been slowly changing to new on-line monitoring techniques for electrical equipments [2, 3, 10, 12, 13, 17, 25, 28, 31]. One of these new methods is the monitoring of the stator current. In this context Martelo [17] and Schoen et al. [25] study bearing failures based on the Fast Fourier Transform (FFT) analysis. Using the same tool, Benbouzid et al. [2] and Cameron et al. [3] analyze other types of failures such as rotor slot effect, saturation, and static and dynamical eccentricities.

At the Electrical Engineering Department of the University of Chile, Gallardo [6], Barrios [1] and González [7] have developed a phenomenological model to simulate broken bars in the rotor of an induction motor and other kind of failures, using as diagnosis methods the short-term Fourier Transform (STFT), multi-resolution analysis (MRA) and also FFT in the transient period.

Regarding failures associated to coil short-circuits in the stator windings, Williamson and Mirzoian [33] developed a model to simulate this type of failure analyzing the positive and negative sequence components of the stator current. Unfortunately, the model requires a large number of parameters, which were obtained after performing a large number of tests on the machine at different operating temperatures. Penman et al. [22] propose a methodology of fault detection based on the analysis of the machine axial flux using FFT. Sottile and Kohler [27] present a fault detection method using the negative sequence component obtained by decomposing the stator current into the symmetric components, getting good practical results. However, Tallan et al. [29] showed that this result is not always reliable, since the negative sequence is present not only when there is coils short-circuit in the stator winding but also when there is a voltage unbalance. Toliyat and Nandi [32] suggest a diagnosis of coil short-circuits by monitoring certain rotor slot related harmonics at the terminal voltage of the machine once it is switched off. In the absence of supply voltage, issues like voltage unbalance or the presence of other harmonics due to frequency converters do not affect the measurements. Although useful, the method cannot be applied on-line.

Lazarevic and Petrovic [14] use wavelets and the decomposition of the stator current to detect broken bars, but instead of using the envelop of the detail coefficients, these are squared to suppress electric noises, obtaining good results when comparing a sane and a failed motor. Combastel et al. [4] apply wavelets to the stator current to detect broken bars and coil short-circuits on the basis of models of the motor based on Park transformation.

Ross [24] and Montanari et al. [19] apply the Weibull distribution to insulation failures and they propose the estimation of α and β parameters, in order to predict breakdown events of the machine insulation, using maximum likelihood (ML)

G. A. Jiménez · A. O. Muñoz · M. A. Duarte-Mermoud (✉)
Electrical Engineering Department,
University of Chile, Av Tupper 2007
Casilla Santiago 412-3, Chile
E-mail: mduartem@cec.uchile.cl

and linear regression (LR) methodology. Yacizi and Kliman [34] propose a statistical following of the motor failures on the rotor and bearings but assuming a Gaussian distribution and using the STFT, to avoid confusing certain machine states with an incipient failure.

The main objective of this paper is to propose a method that is able to detect incipient failures in electrical machines by analyzing the steady sate stator current (such as broken bars, saturation, eccentricities, and bearing failures) or coil short-circuits in the stator windings, if the axial flux is available. The approach is based on the extraction of the envelop of the signal to be analyzed using Hilbert transform, pre-multiplied by a Tukey window to avoid transient distortion. Next, a wavelet analysis similar to that proposed by Lazarevic and Petrovic [14] is performed, but now the effects of the transient are attenuated making the diagnosis a lot easier. Since a failure can be intermittent or can be associated to certain load levels, it is proposed to perform a statistical analysis, like the one proposed by Yacizi and Kliman [34], to determine fault thresholds. In this case the Weibull distribution is used and its parameters α and β are estimated computing the mean value and the standard deviation, and these are used to estimate the fault thresholds.

The paper is organized so that in Sect. 2 the envelop analysis is presented and in Sect. 3 the use of the wavelet analysis is illustrated. Sect. 4 is devoted to the analysis of the experimental data obtained from two motors mounted in the laboratory. In Sect. 5 a statistical analysis based on the Weibull distribution is presented and in Sect. 6 the proposed scheme to detect incipient failures is illustrated using data obtained from industrial measurements. Finally, in Sect. 7 some conclusions are drawn.

2 Hilbert transform and envelop analysis as a tool for fault detection in induction motors

In this section it is demonstrated that the Hilbert transformation of the original stator current signal followed by the spectrum analysis of the envelope of its analytic signal is a useful tool for fault detection in electric motors [9,10,14].

We will first recall the Hilbert transformation of a function of time and then the concept of *analytic signal* is introduced. Next, the *envelop* is obtained as the absolute value of the analytic signal and the *envelop spectrum* is obtained by taking the FFT [15,26] of the envelop. We will refer to this analysis as *envelop analysis* or *envelop spectrum analysis* and it will be compared with the so called *classical analysis* or *classical spectrum analysis* where the *spectrum* (FFT) is computed directly from the original function of time.

This methodology is applied to the analysis of a model of a stator current signal for a motor with a broken bar (failed) and compared with the analysis of a model of a stator current corresponding to a normal motor (sane). Also, this comparative analysis is performed for signals experimentally obtained in the laboratory from two identical motors; one normal and one with a broken bar (See Appendix). In both cases it is found that the frequency spectrum of the envelope is shifted in 50 Hz.

Although only the failure associated with a broken bar is analyzed in this paper, the methodology can be used for many other types of failures through the analysis of the steady state stator current, such as bearing failures, saturation and eccentricities, and also coil short-circuits in the stator winding (through the axial flux signal) [9,10].

2.1 Hilbert transform

Le us consider a real time signal $x(t)$. The *Hilbert transform* $y(t)= H$ x(t) is defined as [16]

$$y(t) = \frac{1}{\pi}\int_{-\infty}^{\infty} \frac{x(\tau)}{\tau - t}\mathrm{d}\tau \tag{1}$$

Using the mean value Theorem we can evaluate (1) to get

$$y(t) = \frac{1}{\pi t} * x(t) \tag{2}$$

Therefore, $y(t)$ is obtained as the convolution between the function $1/\pi t$ and the original signal $x(t)$ Since the Fourier Transform of $1/\pi t$ is

$$F\left(\frac{1}{\pi t}\right) = -j\mathrm{sgn}(f) = \begin{cases} -j & \text{if } f > 0 \\ j & \text{if } f < 0 \end{cases} \tag{3}$$

where f is the frequency in Hertz, this means that the positive frequencies of the spectrum of $x(t)$ are shifted by –90° and the negative frequencies are shifted by 90°. The Hilbert transform can then be viewed as a filter of amplitude unity and phase $\pm 90^\circ$ depending on the sign of the frequency of the input signal spectrum.

When a real signal $x(t)$ and its Hilbert transform $y(t) = H\{\mathrm{x(t)}\}$ are used to form a new complex signal defined as [16]

$$z(t) = x(t) + jy(t) \tag{4}$$

then the signal $z(t)$ is called the a *nalytical signal* associated with $x(t)$. The signal $z(t)$ has the property that all the negative frequencies of $x(t)$ have been filtered.

2.2 Envelope analysis: a new formulation of the fault frequency

The *envelope* $E(t)$ of a complex signal $z(t)$ is defined as

$$E(t) = |z(t)| = |x(t) + jy(t)| \tag{5}$$

that is, the absolute value of the analytical signal defined in (4). To understand better this concept let us compute the envelope of the model of the stator current of a motor presenting a broken bar in its rotor. The spectrum of such signal presents a peak at frequency 2sf and can be modeled as [9,10]

$$I(t) = A\mathrm{sen}(\omega t) + B\mathrm{sen}[(\omega + 2s\omega)t]$$

where s is the slip and f is the frequency in Hertz. The analytic signal associated with $I(t)$ is $z(t) = I(t) + jI_y(t)$,

where $I_y(t) = H\{I(t)\}$ denotes the Hilbert Transform of $I(t)$. Since

$$I_y(t) = -A\cos(\omega t) - B\cos[(\omega + 2s\omega)t] \tag{6}$$

then $z(t)$ is

$$\begin{aligned} z(t) &= -jA\mathrm{e}^{j\omega t} - jB\mathrm{e}^{j2s\omega t}\mathrm{e}^{j\omega t} \\ &= -j\mathrm{e}^{j\omega t}\left[A + B\mathrm{e}^{j2s\omega t}\right] \end{aligned} \tag{7}$$

Finally, the absolute value of $z(t)$ (the envelope) is given by

$$E(t) = |z(t)| = \left|A + B\mathrm{e}^{j2s\omega t}\right| \tag{8}$$

From (8) it can be clearly seen that the fundamental frequency is no longer present but we have the double of the slip frequency ($2s\omega$). Thus, the failure frequency is now represented by peaks at $\pm 2s\omega$ in the spectrum of the envelope and no longer at $\omega \pm 2s\omega$, as in the classical spectrum analysis of the original signal. We can state that the envelope is the magnitude of the sum of the amplitude of the fundamental component A and the phasor B oscillating at the failure frequency $2s\omega$. In Table 1 and Fig. 1 it is shown the values of the expression (8) for different values of $2s\omega t$.

From Fig. 1 it is observed that the variation corresponds to a sinusoid of frequency $2s\omega$ around the fundamental component of magnitude A. Moreover, it can be concluded that the importance of the envelope analysis, as compared with classical spectrum analysis of the original signal, is that it allows to suppress the component with fundamental frequency and to work with failure frequencies, making easier the fault detection process.

Table 1 Variation of the magnitude of the envelope (2.8)

$2s\omega t$	$\lvert E\,(t)\rvert$
0	A+B
$\pi/2$	$\sqrt{A^2 + B^2}$
π	A−B
$3\pi/2$	$\sqrt{A^2 + B^2}$
2π	A+B

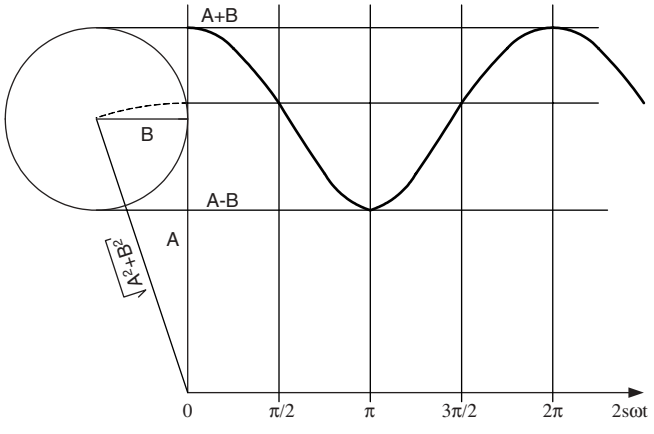

Fig. 1 Envelope of the stator current for a motor with a rotor broken bar

Finally, the previous analysis was done for Eqs. (6–8) which represent an idealized case. This is done only to illustrate how the method works in the ideal case and in the next section the method is used in real oscillograms with distorted waveforms.

2.3 Interpretation in the frequency spectrum

In what follows we will apply the classical spectrum analysis and the envelope analysis to the stator current signals obtained experimentally from two identical motors; one normal and one having a broken bar in its rotor. The signals were obtained from two 5.5 HP motors whose nominal characteristics are described in the Appendix and obtained by González [7]. The signals for the failed motor were registered using a sampling frequency of 10 KHz, allowing analyzing up to a maximum of 5 KHz with a frequency resolution of 0.25 Hz, whereas for the normal motor a sampling period of 5 KHz was used, which means an analysis up to 2.5 KHz [51].

In Figs. 2–5, the differences between both methodologies can be appreciated, the analysis being more precise when using the envelope spectrum of the stator current (Fig. 5) as compared with the classical spectrum analysis (Fig. 3). Figure 2 shows the original current signal of phase '*a*' for the motor under failure, whereas in Fig. 3 its Fourier transform (power spectrum) it is shown. Figure 4 shows the envelope of the original signal Fig. 2, computed according to (8). Finally, the power spectrum of the envelope plotted in Fig. 4 is shown in Fig. 5. From Figs. 3 and 5 it can be seen that the spectral analysis of the envelope is simpler than the spectral analysis of the original signal to identify failure frequencies. Note that when the Hilbert transform is used, it is necessary to look for the frequency ± 2sf (Fig. 5) and not for 50 ± 2sf, as in the classical spectrum analysis (Fig. 3).

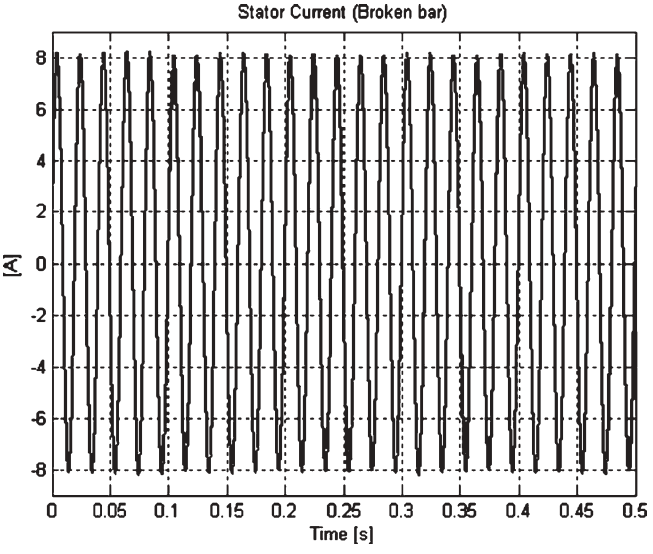

Fig. 2 Stator current for the motor under failure

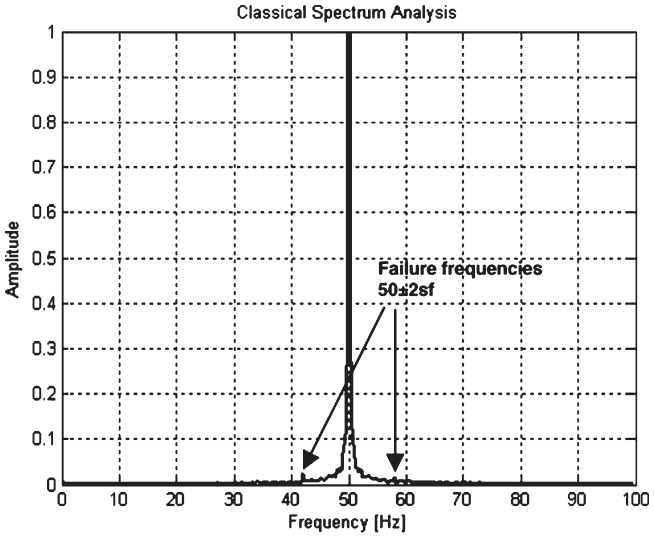

Fig. 3 Spectrum of the stator current for the motor with a broken bar

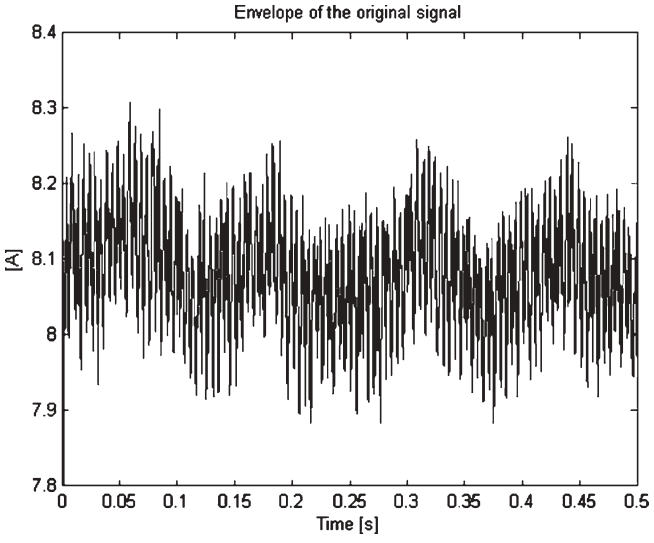

Fig. 4 Envelope of the stator current for the motor under failure

The methodology that uses the power spectrum of the envelope of the original stator current signal has been shown here for detecting a failure corresponding to a broken bar in the rotor. However, the same methodology can also be used to analyze other type of motor failures such as saturation and eccentricities, bearing failures, coil short-circuits in the stator windings and their combinations. A detailed analysis of these types of failures and the corresponding failure frequencies associated with this methodology can be found in [9, 10].

3 Wavelets and its application to fault detection

Wavelets analysis allows representing functions of time satisfying certain mathematical requirements [4,5,11,14,18,20,

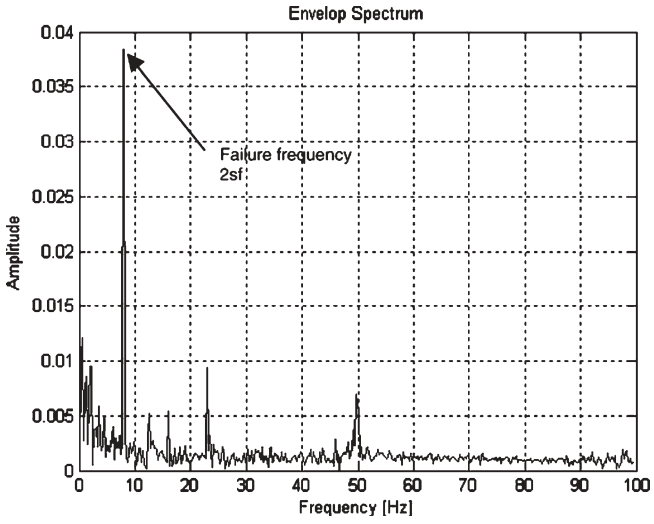

Fig. 5 Spectrum of the envelope of the stator current for the failed motor

21,30]. Unlike Fourier analysis, in wavelet analysis the scale used to analyze the signal plays an important role. In wavelet analysis, the signals are processes at different scales or resolutions. Thus, if we look at the signal with a wide window, we will identify general characteristics, whereas if a small window is used then we obtain detailed information about it [21]. Another important feature that makes wavelets interesting is that they allow the analysis of choppy and non-stationary signals.

3.1 Continuos wavelet transform

Unlike Fourier transform, the technique based on wavelets allows to perform, through a multi-resolution analysis (MRA), several overlapped projections of the signal. For a signal $f(t)$ the *generating function* of the MRA can be expressed as [18]

$$\varphi_k^j(t) = 2^{-j/2}\varphi(2^{-j}t - k) \tag{9}$$

where φ is the so called *mother wavelet, j* indicates the *decomposition level* and k is the *time shift* factor. The wavelet coefficients obtained by applying an orthogonal wavelet are [18]

$$d_k^j = \int_{-\infty}^{\infty} f(t)\psi_k^j(t)\mathrm{d}t \tag{10}$$

where ψ_k^j is the *wavelet analyzing function* obtained from φ. For example, Haar, Morlet, Shannon, etc. could be used.

3.2 The discrete wavelet: multi-resolution analysis (MRA)

Let $s(n)$ be a discrete-time signal to be decomposed into its approximate and detailed versions using the MRA. The first level decomposition coefficients are $a_1(n)$ and $d_1(n)$, where $a_1(n)$ is the approximate version of the original signal $s(n)$ and $d_1(n)$ is the detailed representation of the original signal $s(n)$ which are defined as [5],

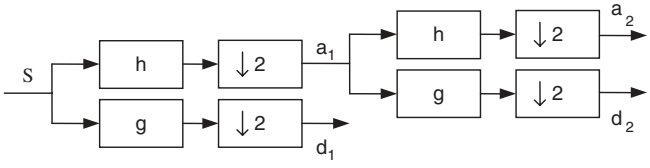

Fig. 6 Multi-resolution analysis (MRA) decomposition algorithm

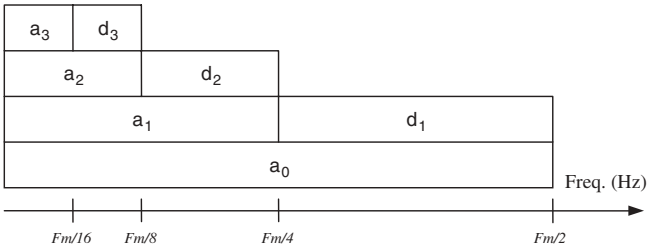

Fig. 7 Scale and frequency dependence of the wavelets

$$a_1(n) = \sum_k^n h(k-2n)s(k)$$
$$d_1(n) = \sum_k^n g(k-2n)s(k) \quad (11)$$

where $h(n)$ and $g(n)$ are the decomposition filters of $s(n)$ in $a_1(n)$ and $d_1(n)$, respectively. The next (second) decomposition level is based on $a_1(n)$ and the coefficients are given by [5],

$$a_2(n) = \sum_k^n h(k-2n)a_1(k)$$
$$d_2(n) = \sum_k^n g(k-2n)a_1(k) \quad (12)$$

Upper level decompositions can be obtained in a similar fashion. The coefficients a_j and d_j are computed using the tree decomposition algorithm allowing storing low frequency information of the signal as well as the discontinuities.

In Fig. 6 [4] h, g, represent the decomposition filters and $\downarrow 2$ denotes a down sampling by a factor of 2. Thus, we can conclude that $a_1(n)$ being the approximate version of the original signal, $h(n)$ behaves as a low pass filter. If $d_1(n)$ contains only high frequency components of signal $s(n)$, then $g(n)$ behaves as a high pass filter.

Detailed and approximate coefficients of a signal are related to its spectral content. The MRA performs a dilatation of the spectrum towards the low frequencies, as shown in Fig. 7 [4]. That is why by analyzing the spectrum of the approximate and detailed coefficients at a higher level, the spectral content of the signal can be analyzed [5].

3.3 Application to fault diagnosis

The first consideration before applying the MRA algorithm to obtain good signal decomposition, is the selection of the most suitable wavelet for the desired purposes. There is no clear criterion to select the most adequate wavelet, but it is convenient to use only one type of wavelet for the whole decomposition process.

It is also recommended to use high decomposition levels (greater than four). For lower levels the mother wavelet is located more in time and oscillates faster in a short period of time. As the wavelet goes to higher levels, it is located less in time and oscillates less due to the dilatation nature of the wavelet transform. Therefore, fast and low type of faults can be detected with one type of wavelet.

A practical suggestion is to use a wavelet "similar" to the nature of the perturbation to be analyzed. In this study we have chosen the wavelet Symlet 8 [5]. Symlet is a family of wavelets that are almost symmetric and were proposed by Daubechies as a modification to the family of Daubechies wavelets (db). Both families have similar properties.

4 Experimental results

In what follows we will apply the MRA procedure to the stator current signals obtained experimentally in the laboratory from two identical motors; one normal and one having a broken bar in the rotor, as described in Sect. 2.3 [7].

4.1 Application of the MRA

The MRA was carried out decomposing the original current signals into 10 levels, each one of them having its own detailed coefficients and a determined range of frequencies, as shown in Tables 2 and 3 for a motor under failure and one without failure, respectively.

The MRA of the stator current for both motors was done using the MATLAB Wavelet Toolbox, where the wavelet Symlet 8 with 10 decomposition levels was selected [4]. At the seventh level we could find important differences for the failed motor, since it contains the frequency components $f \pm 2sf$, which in this case are 42 and 58 Hz (see Table 2). The same is also true at the sixth level for the sane motor (see Table 3).

Table 2 Multi-resolution analysis (MRA) decomposition levels for the motor under failure

Level	Frequency range [Hz]	
	From	To
1	5,000	2,500
2	2,500	1,250
3	1,250	625
4	625	312.5
5	312.5	156.25
6	156.25	78.12
7	78.12	39.06 (50±2sf = 42, 58)
8	39.06	19.53
9	19.53	9.76
10	9.76	4.88 (2sf = 8)

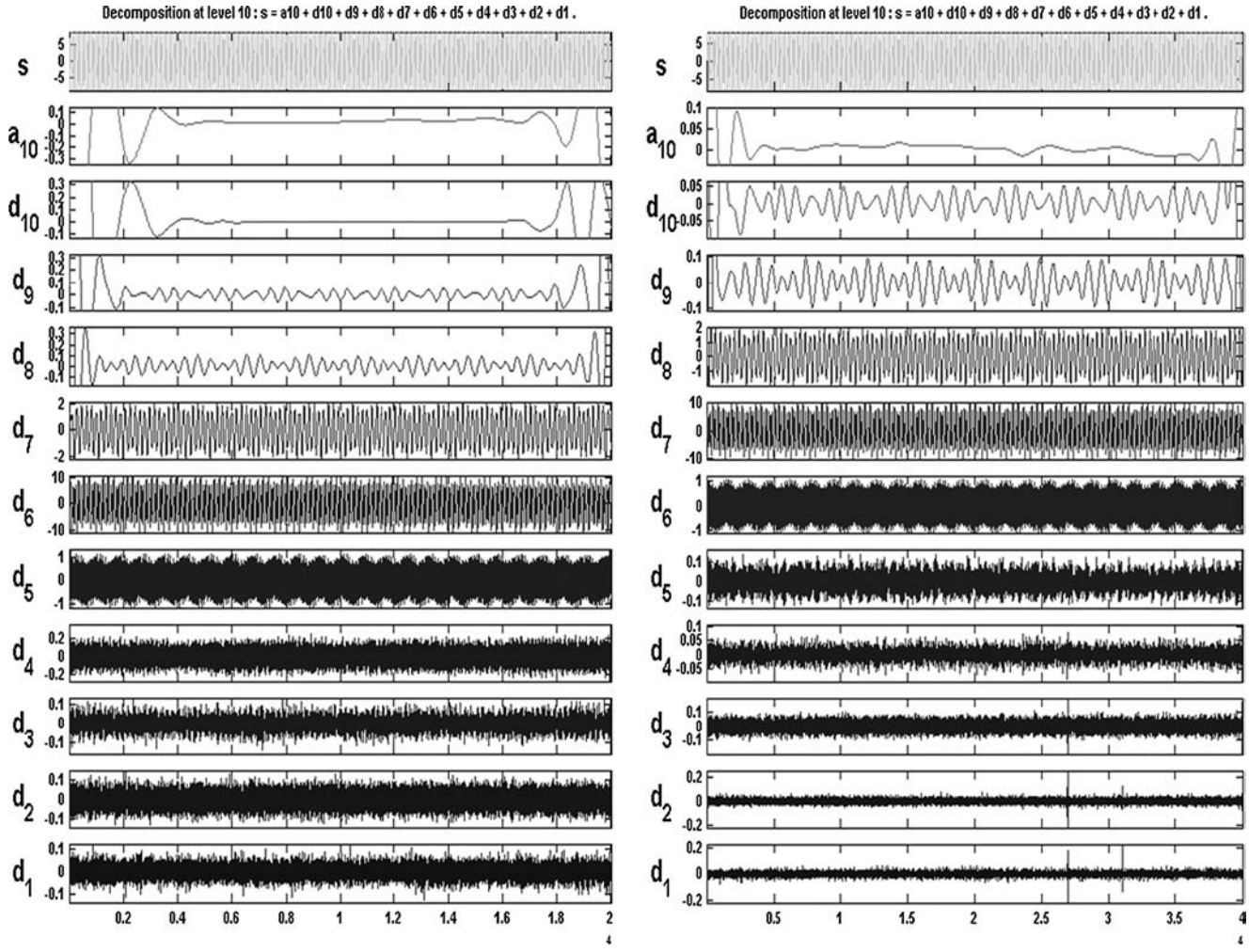

Fig. 8 Level decompositions for a sane motor (*left*) and one with a broken bar in the rotor (*right*). Notice the differences between the seventh level (fault) and sixth level (sane)

Table 3 MRA decomposition levels for the sane motor

Level	Frequency Range [Hz]	
	From	To
1	2,500	1,250
2	1,250	625
3	625	312.5
4	312.5	156.25
5	156.25	78.12
6	78.12	39.06 ($50 \pm 2\text{sf} = 42, 58$)
7	39.06	19.53
8	19.53	9.76
9	9.76	4.88 ($2\text{sf} = 8$)
10	4.88	2.44

In Fig. 8 we can see the comparison of the total decomposition between both signals and in Fig. 9 we can compare the detail coefficients corresponding to the seventh level for the failed motor and for the sixth level for the sane motor.

Although there are differences of the detail coefficients for the failed motor, it is not convenient to directly compare both of them, since at these levels the fundamental component (50 Hz) plays an important role and it is present in the whole analysis.

Due to the above inconvenience, the same procedure was followed for the envelops of both signals, taking first the Hilbert transform, to eliminate the fundamental component in both signals.

Figure 10 shows the decomposition for the envelope of the signals coming from the failed and sane motors. Now we have to look for the frequency 2sf, i.e. 8 Hz in this case. Therefore, according to Tables 2 and 3, we have now to pay attention at the tenth level for the failed motor and at the ninth level for the sane motor. For a better comparison, the detailed coefficients of both the above mentioned levels are illustrated in Fig. 11.

The differences between Figs. 9 and 11 are evident when comparing the appropriate levels for both motors. In Fig. 11 the transient exhibited at the beginning and at the end of the decomposition is due to the filter used for realizing the decomposition. For a better comparison it is preferable to compare the envelopes of the signals as shown in Fig. 12, instead of the detail coefficients shown in Fig. 8.

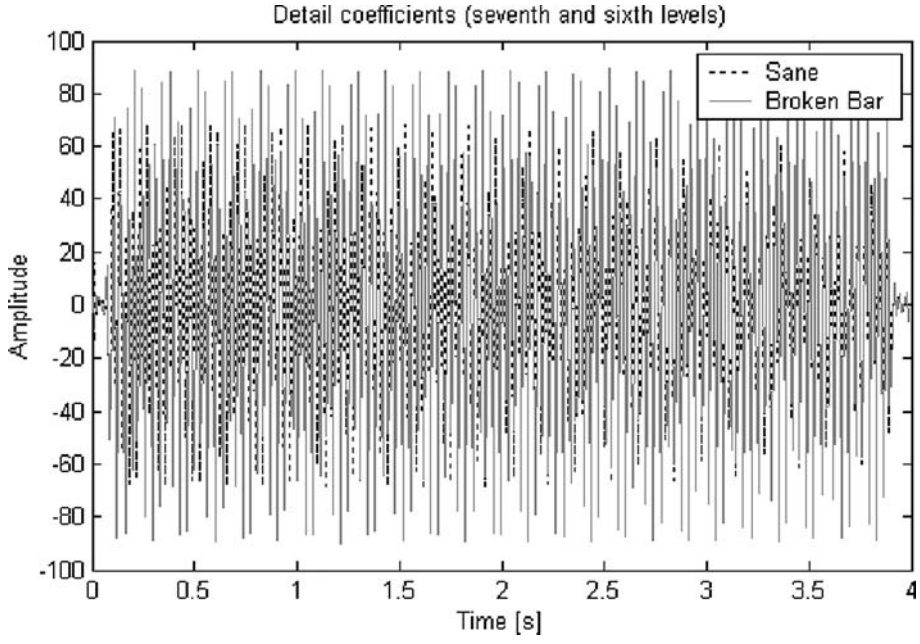

Fig. 9 Comparison between the signals for the failed and sane motors, corresponding to the seventh and sixth levels, respectively

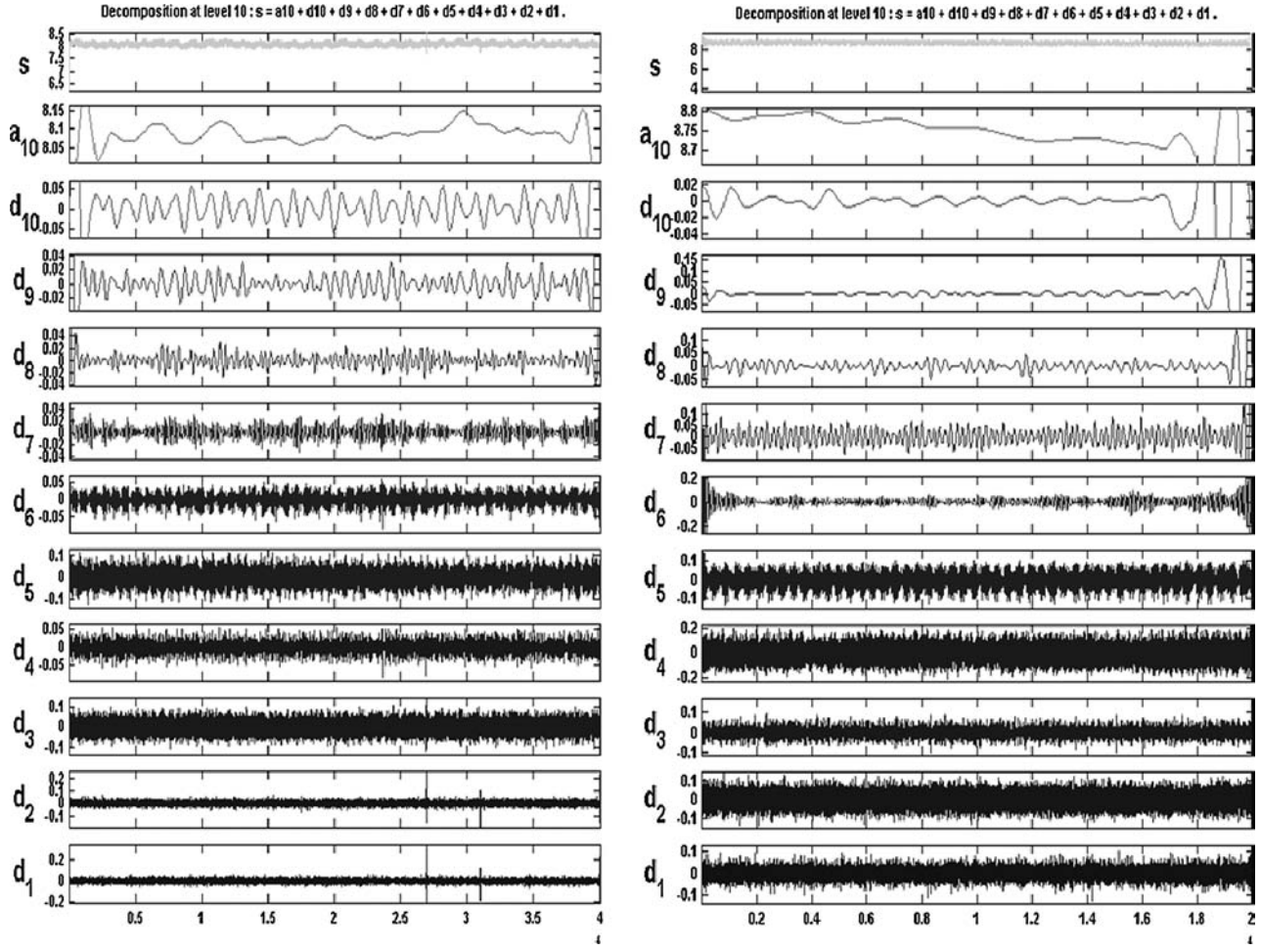

Fig. 10 Wavelet decomposition of the envelops of the stator current for a sane motor (*right*) and one with fault (*left*). Notice the difference between the ninth level (sane) and the tenth level (fault)

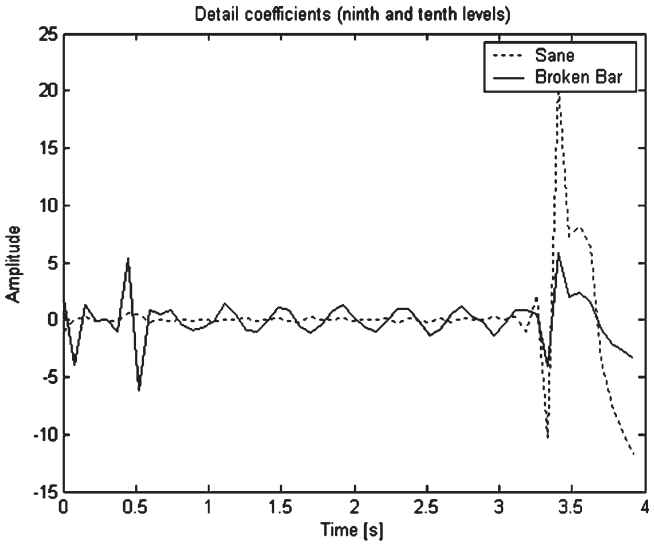

Fig. 11 Detail coefficients of the envelop decomposition for the sane motor (ninth level) and failed motor (tenth level)

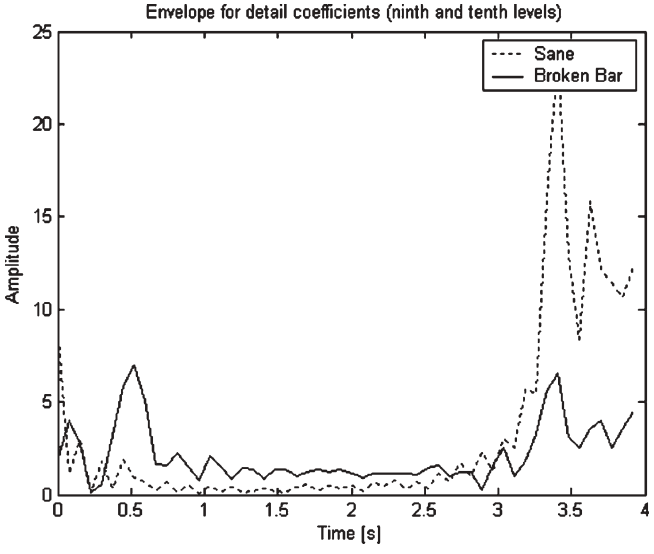

Fig. 12 Envelopes of the detail coefficients (Fig. 4.4) corresponding to the ninth level (sane) and tenth level (failed)

4.2 Transient suppression

The MRA carried out in the previous section allows a better comparison between the failed and sane motors. It can be noticed from Figs. 11 and 12 that the values should be close to those observed between 1 and 3 s, but the transient does not allow getting clearer results. For this reason a window was used to pre-multiply the envelope in order to suppress the transient effects. A Tukey window was selected which is of the cosine type graduated according to the parameter α. When $\alpha \leq 0$, the window becomes rectangular and when $\alpha \geq 1$ it becomes a Hanning window. Figure 13 shows the form of the Tukey window for different values of α [30].

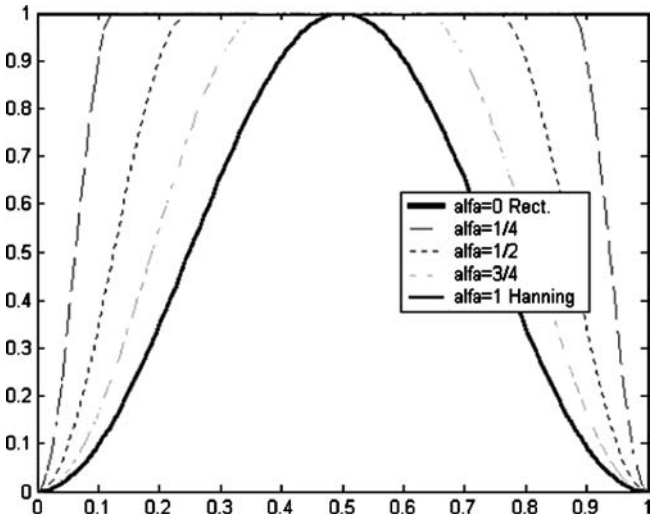

Fig. 13 Form of the Tukey window for different values of α

In this study, a value of $\alpha = 0.225$ was chosen and the envelope was pre-multiplied by this Tukey window. Then the detailed coefficients were computed for the ninth level (sane motor) and tenth level (failed motor) suppressing successfully the transients as shown in Fig. 14.

Comparing Figs. 11 and 12 with Fig. 14 it is evident the improvement obtained by suppressing the transient in the wavelet decomposition allows a better comparison between the sane and failed motors and hence a better fault diagnosis.

To complete the failure analysis, it remains to estimate the fault threshold. To this extent statistical analysis will be used in the next section to determine trends and mean values.

5 Weibull distribution as a tool for fault detection

In order to complete the fault diagnosis process, a methodology is proposed to estimate the expected mean values for each level where a fault is present. Thus, a more reliable comparison can be done to establish failure thresholds. To perform this estimation the Weibull distribution was chosen. Unlike other probability distributions, this distribution allows us to observe the displacement of the mean value when the motor goes from a state without failure to a state under failure.

5.1 The Weibull distribution

The probability distribution and density functions for a Weibull distribution are given by

$$F(x;\alpha,\beta) = 1 - \mathrm{e}^{-\left[\frac{x}{\alpha}\right]^{\beta}} \tag{13}$$

$$f(x;\alpha,\beta) = \frac{\beta}{\alpha}\left[\frac{x}{\alpha}\right]^{\beta-1}\mathrm{e}^{-\left[\frac{x}{\alpha}\right]^{\beta}} \tag{14}$$

where α is the *scale parameter* and β is the *shape parameter*. The Weibull distribution is used to describe cases where

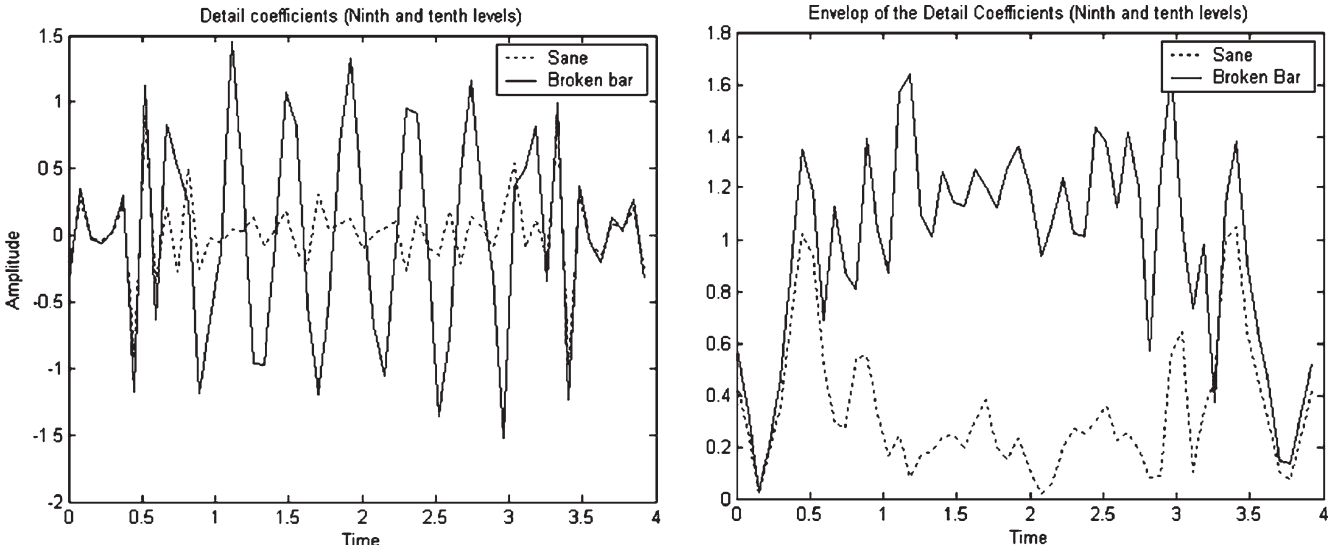

Fig. 14 Comparison of the detailed coefficients (*left*) and their envelopes (*right*) once the Tukey window was applied

a small value of a parameter determines the behavior of the whole system [24]. Since they are normally unknown, the parameters α and β of the Weibull distribution have to be estimated from the current signals. In this study we will use the ML method to estimate α and β [24]. Their estimates will be denoted as a and b, respectively.

The ML method will be used in this study because its insensitivity to data dispersion and moderate computational resources. The method is based on the optimization of the likelihood function $L(a, b, X_i)$, or its logarithm, defined as [24]

$$\begin{aligned} \ln L(a,b;X_i) &= \sum_{i=1}^{n} \ln f(X_i;a,b) \\ \ln L(a,b;X_i) &= n\ln b - n\ln a \\ &\quad +(b-1)\sum_{i=1}^{n}\ln\frac{X_i}{a} - \sum_{i=1}^{n}\left[\frac{X_i}{a}\right]^{\beta} \end{aligned} \tag{15}$$

The estimates a and b are obtained through the maximization of L, or more conveniently $\ln L$. This leads to the following conditions [24]

$$\frac{\partial \ln L}{\partial a} = \frac{\partial \ln L}{\partial b} = 0 \tag{16}$$

Assuming the data follows a Weibull distribution the above conditions become

$$\frac{\sum_{i=1}^{n} X_i^b \ln X_i^b}{\sum_{i=1}^{n} X_i^b} - \frac{1}{n}\sum_{i=1}^{n}\ln X_i^b = 1, \tag{17}$$

which has no analytic solution and has to be solved numerically, typically using the Newton-Raphson method, finding the estimate b. The estimate a is obtained by replacing b in the following equation

$$a^b = \frac{1}{n}\sum_{i=1}^{n} X_i^b \tag{18}$$

It is known that the ML method estimate has a bias [24]. The bias depends on the size of the sample and the degree of censoring. Recently, two methods have been proposed to reduce the bias in the shape estimate b for the case of uncensored data. One is based on pivotal functions [23] and other on a relative (or generalized) likelihood function [8]. In this study we will use the methodology based on pivotal functions. Thus, a function b_U is used to obtain a better estimate of b. The chosen function here is [24]

$$b_U = \frac{n-2}{n-0.68}b \tag{19}$$

where n is the number of data. This expression reduces the bias typically to less than 0.3% of β [24].

In order to determine the fault threshold we shall compute the means value $\bar{T}$ and the standard deviation σ. The mean value (MV) for the Weibull distribution is given by

$$\bar{T} = \alpha \cdot \Gamma\left(\frac{1}{\beta}+1\right) \tag{20}$$

where $\Gamma\left(\frac{1}{\beta}+1\right)$ is the Gamma function evaluated in $\left(\frac{1}{\beta}+1\right)$. The standard deviation (SD) is given by

$$\sigma = \alpha\sqrt{\Gamma\left(\frac{2}{\beta}+1\right) - \Gamma\left(\frac{1}{\beta}+1\right)^2} \tag{21}$$

5.2 Experimental verification of the estimates

Now we shall use the information contained in the stator currents for the two 5.5 HP motors described in Sect. 2.3 and in the Appendix, obtained by González [7]. In Sect. 4, the information of the envelope of the detail coefficients was obtained through wavelet analysis. Using this information for the level where the fault is located (tenth) and assuming a Weibull distribution, we shall estimate the MN and the SD.

From the results shown in Sect. 4 we define two vectors of dimension 54, one for the envelope in the ninth channel (sane motor) and one for the envelope in the tenth channel (failed motor). Ten frequency intervals were selected and the histogram for each motor was built, as shown in Tables 4 and 5. The same information is shown in Figures 5.1 and 5.2.

From Tables 4 and 5, and Figs. 15 and 16 it can be seen that there is a trend towards the value 0.3 for the sane motor and to a value close to 1 for the failed motor (broken bar). This coincides with the envelopes obtained in Fig. 14.

The next step in the analysis is to estimate the probability distribution function (i.e. the α and β parameters) for both cases. In order to get a good estimation of β we use the ML method with the pivotal function b_U described in (19). Table 6 shows the function, number of samples and errors obtained in the numerical solution of Eq. 17 by the Newton–Raphson method.

Once a and b are obtained, the distribution and density probability functions are computed, also the mean value estimate (MVE) and the standard deviation estimate (SDE) are calculated. These are shown in Table 7.

In Figs. 17 and 18 are plotted the probability density function and the probability distribution function for both motors. The density functions are in complete agreement with the information contained in the histograms, obtaining for the sane motor an MVE of 0.3358 and for the motor under failure an MVE of 0.9585.

Finally, in Fig. 19 the envelops are illustrated together with the MVE. It can be seen that the MVE are in agreement

Table 4 Frequency distribution for the sane motor

Interval number	Mean value interval	Frequency
1	0.0689	10
2	0.1722	10
3	0.2755	15
4	0.3788	5
5	0.4821	4
6	0.5854	3
7	0.6888	3
8	0.7921	0
9	0.8954	1
10	0.9987	3
	TOTAL	54

Table 5 Frequency distribution for the motor with a broken bar

Interval number	Mean value interval	Frequency
1	0.1078	3
2	0.2694	3
3	0.4311	3
4	0.5927	4
5	0.7543	3
6	0.916	6
7	1.0776	13
8	1.2392	9
9	1.4008	7
10	1.5625	3
	Total	54

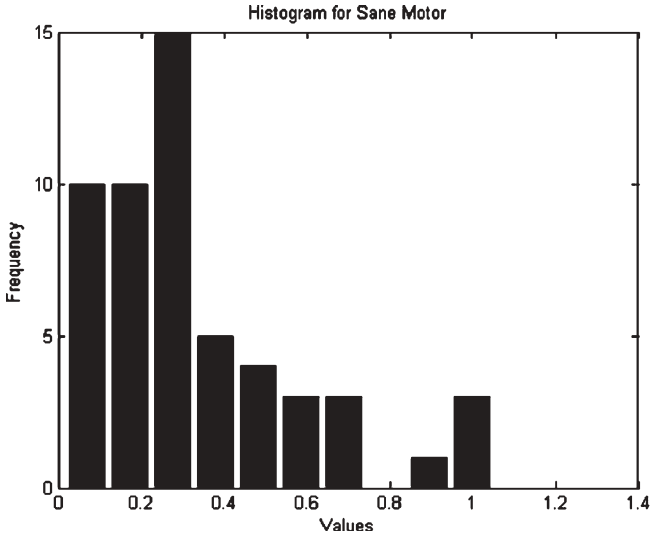

Fig. 15 Histogram for the sane motor

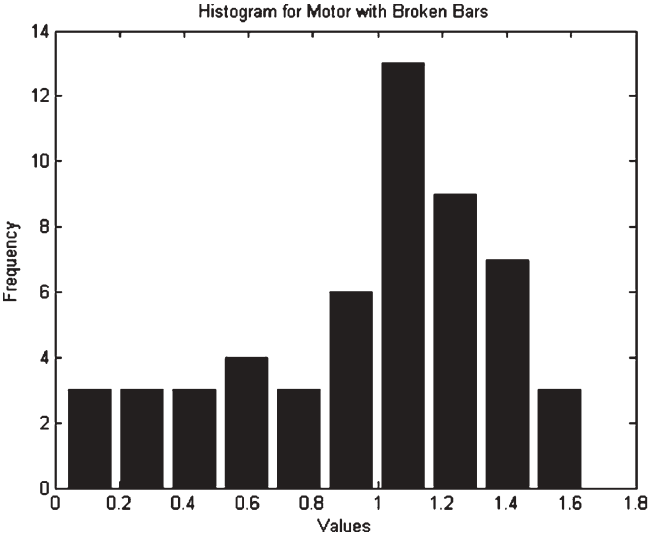

Fig. 16 Histogram for the motor with a broken bar

Table 6 Pivotal function and convergence errors in the Newton–Raphson method

Total data number (n)	b_U	Error sane motor	Error failed motor
54	0.9752b	2.463E-04	1.011E-06

Table 7 Statistical parameters for a sane motor and a failed motor *MVE* mean value estimate; *SDE* standard deviation estimate

Parameter	Sane motor	Failed motor
α	0.3698	1.0794
β	1.4361	2.576
MVE	0.3358	0.9585
SDE	0.2373	0.3993

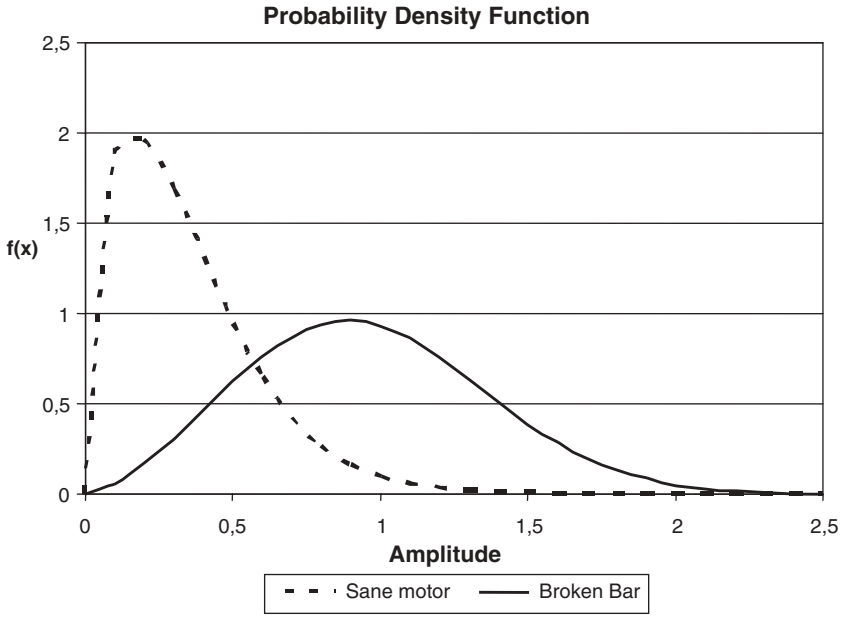

Fig. 17 Probability density function for the envelopes of the detailed coefficients

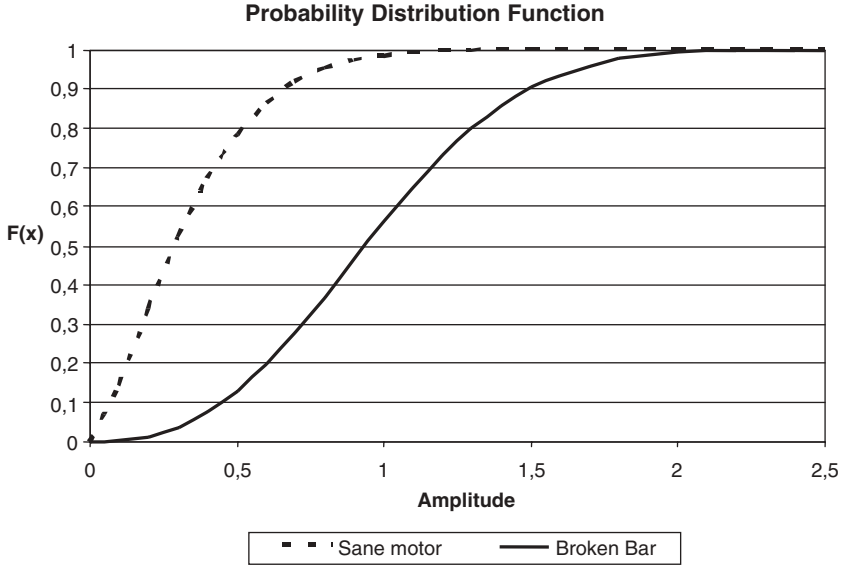

Fig. 18 Probability distribution function for the envelopes of the detailed coefficients

with those of Figs. 17 and 18. Though it is not possible to completely suppress the transient effect, the result is quite satisfactory

This fact will allow monitoring on-line the MVE for both motors and performing an incipient diagnosis of a broken bar in the rotor. For example, when the motor is in good condition (sane) the evolution of the MVE can be monitored, and if it get closer to one, it would mean that a failure of the broken bar type has occurred or is about to occur. Also, monitoring each frequency level and comparing with predetermined thresholds will allow the reliable diagnosis of incipient failures.

6 A new scheme for incipient fault detection

Based on the results exposed in the previous sections we can now establish a methodology for incipient fault diagnosis in induction motors including broken bars, coil short-circuits, saturation and eccentricities, or bearing failures.

6.1 General methodology

The general block diagram of the proposed methodology is shown in Fig. 20. In this scheme we can distinguish first an

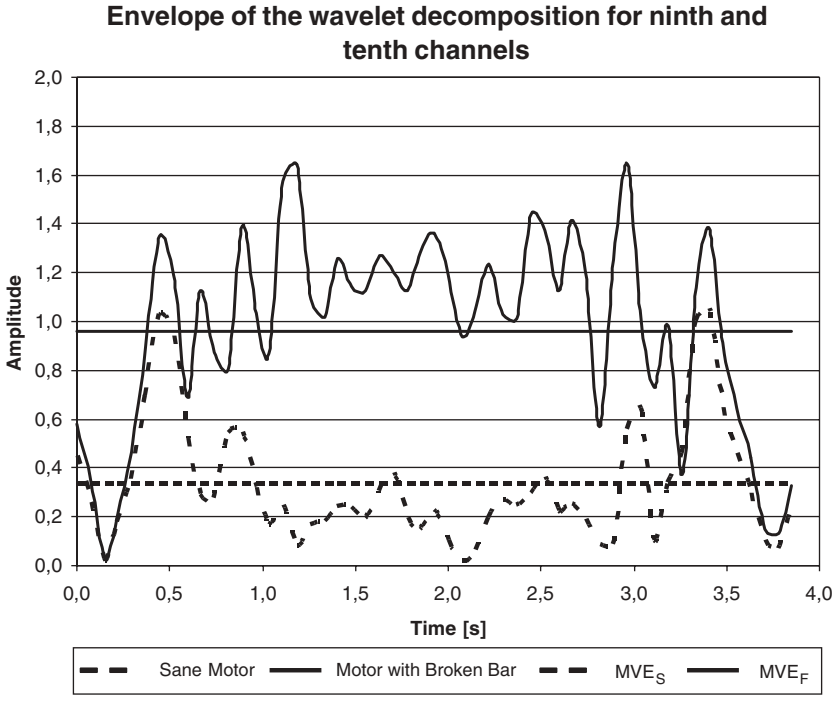

Fig. 19 Envelopes of the details coefficients and their corresponding mean value estimate (MVE)

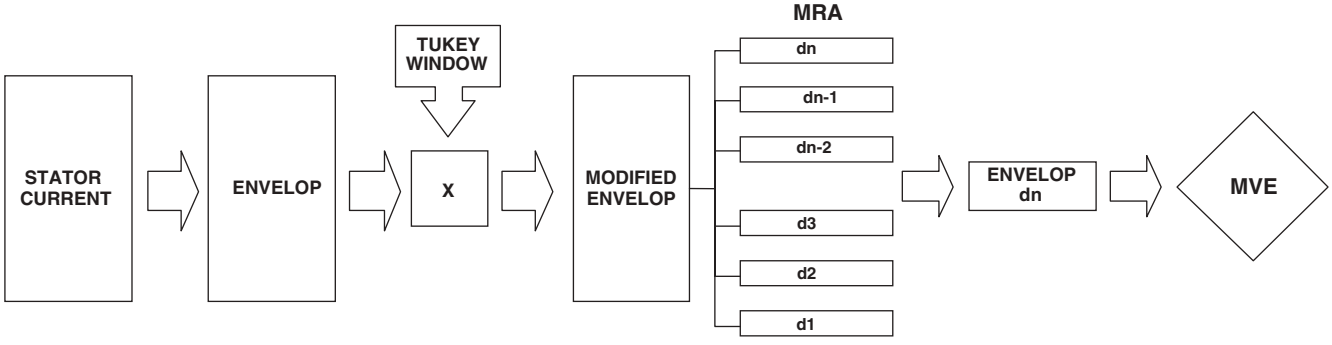

Fig. 20 Block diagram of the methodology for detecting incipient failures

envelope analysis like the one explained in Sect. 2, followed by a transient suppression stage. Next an MRA based on wavelets is applied, ending up with the on-line computation of the MVE.

6.2 Application to real data

We will apply the methodology described in Sect. 6.1 to the case of two induction motors each one of them moving a 600 m conveyor belt located in the Candelaria copper mine, in the III Region of Chile. The ratings of the motors are 1,500 HP, 3.3 kV, 4 poles and 1,485 rpm. The data was obtained by González [7] and we will denote the motors as A and B.

A recording of the stator current for both motors was done in the field while the motors were working under normal conditions. The signals were sampled at a frequency of 1,280 Hz and after the MRA decomposition is done, we get the results shown in Table 8 for each level.

Table 8 Level decomposition for MRA

Level	Frequency range [Hz]	
	From	To
1	640	320
2	320	160
3	160	80
4	80	40
5	40	20
6	20	10
7	10	5
8	5	2.5
9	2.5	1.25
10	1.25	0.6125

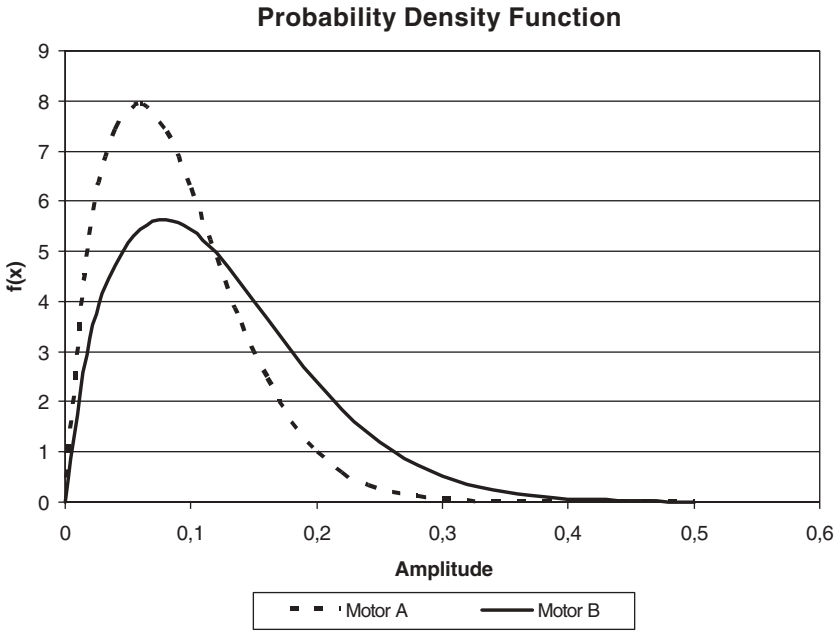

Fig. 21 Probability density function for the envelops of the detail coefficients

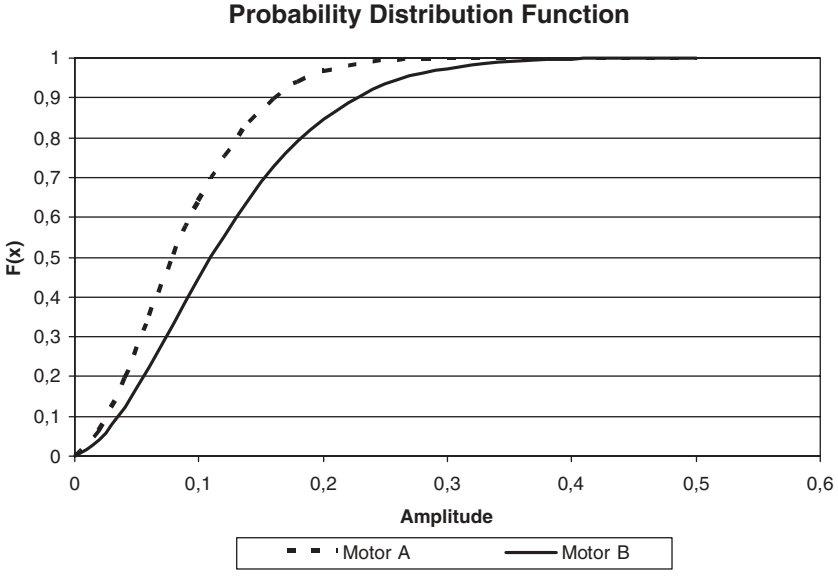

Fig. 22 Probability distribution functions for the envelops of the detail coefficients

Once the general scheme is applied with $\alpha = 0.225$ for the Tukey window, the results are shown in Figs. 21 and 22, where the resulting densities and distributions are plotted for each motor. In Fig. 23 the envelopes with their respective MVE are shown. In Table 9, the values of the parameter estimates are presented.

An incipient failure can be observed at 4 Hz, therefore (according to Table 6.1) the level to observe is the eighth. Although the differences between the two motors are not that noticeable as in the case of the experimental analysis for the two 5.5 HP motors done in Sect. 2.3, there is a clear tendency to a bar breakage in motor B. The diagnosis should suggest then a closer monitoring of the MVE for the motor under suspicion.

Moreover, it is important to mention that the sampling frequency used to register the signal in this case is low (1,280 Hz). It is also suggested to repeat the test with higher sampling frequencies, to obtain more details and to avoid possibly aliasing, then loosing important information.

Finally, as far as the advantages of the proposed method with respect to other methodologies we can state the following:

(a) The method suggested here allows identifying in a much easier way the fault frequencies by suppressing the fundamental.

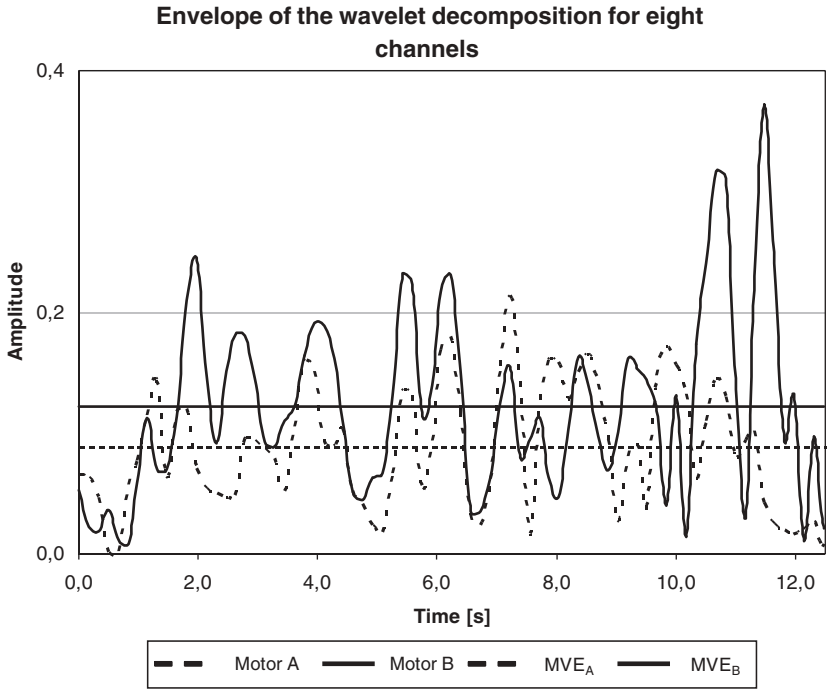

Fig. 23 Envelopes of the detailed coefficients and the corresponding MVE

Table 9 Statistical parameters for motors A and B

Parameter	Motor A	Motor B
α	0.0982	0.1371
β	1.6989	1.6586
MVE	0.0876	0.1225
SDE	0.0531	0.0759

Table 10 Nameplate data for the motors in the experimental set up in the laboratory

	Failed motor	Sane motor
Make	WEG	WEG
Power [HP]	5.5	5.5
Velocity [RPM]	1440	1425
Voltage [V] Δ	380	380
Y	660	660
Current [A] Δ	9.3	8.7
Y	5.4	5.01
Frequency [Hz]	50	50
Insulation class	F	F

(b) Using the proposed method, not only can fault frequencies be detected but also phenomena like saturation and slot effects.
(c) With this methodology there is no need of logarithmic scales as in the direct application of FFT.
(d) The proposed methodology is not based only on one test, but it can be repeated several times giving a certainty to the user that in fact there is a fault.
(e) By using the MRA, the evolution through time of a failure can be observed and analyzed.
(f) In spite of the use of more sophisticated tools in the proposed methodology, its on-line implementation is not difficult.

The main disadvantages of the proposed methodology are:

(a) Although the implementation is not difficult, it requires the use of additional tools (Hilbert Transform, Tukey windows, MRA, etc.), which are not as commonly used in industry as the FFT and Hanning windows.
(b) Handling the transient effects generated by the MRA is dedicated, and a bad choice of the coefficient of the Tukey window can lead to erroneous results.

7 Conclusions

In this paper, the development of a new methodology for incipient fault detection in electrical machines was proposed. The methodology can be implemented on-line and it is based on the envelope concept and analyzing not only the spectrum of the signals (frequency domain analysis) but also analyzing the signals in the time domain by means of the MRA. The statistical method included in the methodology provides the necessary tools to analyze the trends of the fault components and to make a closer following of incipient failures.

The method is valid for analyzing not only steady-state stator current signals to detect broken bars, bearing malfunctioning, rotor slot effects, saturations, and dynamical and static eccentricities, but also the rotor axial flux signal (when available), detecting coil short-circuits in the stator windings,

and analyzing vibration signals to detect bearing failures (the last two types of failures not treated in this paper).

The envelope analysis, with the help of the Hilbert transformation, produced quite satisfactory results. The elimination of the fundamental component allows a clearer identification of the fault frequencies. According to the analysis done in this study, to apply this methodology it is recommended to use a sampling period greater than or equal to 0.25 s.

The multi-resolution analysis is demonstrated to be useful to analyze the failure components through time and not in certain specific points of time. It was observed that this analysis is conveniently performed on the envelope of the detail coefficients but not directly over the stator current. The multiplication of the signal by a Tukey window constitutes another novelty of the proposed approach to eliminate the transient effects, allowing a better comparison at the different decomposition levels between a sane motor and one presenting a failure of the type analyzed here.

Due to the intermittency of the failures, a statistical treatment of the data was suggested to avoid incorrect diagnosis. The Weibull distribution, and the methodology chosen to determine its parameters, allowed establishing failure thresholds, avoiding comparing graphics data and having an index of the state of the machine. Monitoring the MVE is a useful tool that allows more precise judgments about incipient faults, making the fault diagnosis easier, which constitutes another contribution of this work.

Besides the analysis based on models, the proposed methodology was validated with signals obtained in the laboratory and also from data obtained in the field.

As future work, it is necessary to perform studies of much longer duration on machines operating in the laboratory and in the industry in order to evaluate the proposed methodology under different types of failures. Also, new ways of suppressing the effects of the transient is another point for further study to improve the diagnosis of incipient faults using this methodology.

Acknowledgements The results reported in this paper have been partially supported by CONICYT-CHILE through grant FONDECYT N° 1030962.

References

1. Barrios A (1997) Diagnosis of incipient failures in induction machines based on multi-resolution analysis and time-frequency decomposition. (In Spanish). Electrical Engineer Thesis, Department of Electrical Engineering, University of Chile, Santiago, Chile
2. Benbouzid M, Beguenane R, Viera M (1999) Induction motor asymmetrical faults detection using advanced signal processing techniques. IEEE Trans Energy Conver 14(2):146–152
3. Cameron JR, Thomson WT, Dow A (1986) Vibration and current monitoring for detecting air gap eccentricity in large induction motors. IEE Proc 133B(3):155–163
4. Combastel C, Lesecq S, Petropol S, Gentil S (2002) Model-based and wavelet approaches to induction motor on-line fault detection. Control Eng Pract 10(5):493–509
5. Daubechies I (1994) Ten lectures on wavelets. CBMS, SIAM 61:198–202, 254–256
6. Gallardo E (1996) Diagnosis of the electromechanical state of induction motors based on acceleration tests. (In Spanish). Electrical Engineer Thesis, Department of Electrical Engineering, University of Chile, Santiago, Chile
7. González D (1998) Development of patterns for failure recognition in induction motors through recording of transient phenomena. (In Spanish). Electrical Engineer Thesis, Department of Electrical Engineering, University of Chile, Santiago, Chile
8. Jacquelin J (1993) Generalization of the method of Maximum Likelihood. IEEE Trans Electr Insul 28(1):65–72
9. Jimenez GA (2003) Diagnosis of incipient failures in induction motors based on the envelope analysis. (In Spanish). M.Sc. Thesis, Department of Electrical Engineering, University of Chile, Santiago, Chile
10. Jimenez GA, Munoz A, Duarte M (2003) A new scheme for the analysis of failures in induction motors based on the measurement of the stator current. (In Spanish). In: Proceedings of the 10 Latin American regional workshop of CIGRE, May 18–22, 2003, Puerto Iguazú, Argentina. Proceedings in CD, Track No. 11–27, 6 pp
11. Kaiser G (1994) A friendly guide to wavelets. Department of Mathematics, University of Massachusetts. Birkhäuser
12. Kliman GB, Premerlani WJ, Yacizi B, Koegl R, Mazereeuw J (1997) Sensorless on line motor diagnostics. IEEE Comput Appl Power 10(2):39–43
13. Landy CF, Walliser RF (1994) Determination of interbar current effects in the detection of broken rotor bars in squirrel cage induction motors. IEEE Trans Energy Conv 9(1):152–158
14. Lazarevic Z, Petrovic D (2000) The advanced method of rotor failure detection in large induction motors. Session 2000 CIGRE 11–203. Paris
15. Lawrence M (1999) Computing the discrete-time "analytic" signal via FFT. IEEE Trans Signal Process 47(9):2600–2603
16. Long D (1998) Comments on Hilbert transform based signal analysis. MERS Technical Report MERS 95–005. Microwave Earth Remote Sensing Laboratory, Department of Electrical and Computer Engineering, Brigham Young University
17. Martelo A (2000) Fault detection of ball bearing in electrical motors by means of vibration, noise and stator current spectral analysis. (In Spanish). M.Sc Thesis, Department of Mechanical Engineering, University of Los Andes, Bogotá, Colombia
18. Meyer Y (1993) Wavelets: algorithms and applications. Society of Industrial and Applied Mathematics, Philadelphia
19. Montanari G, Mazzanti G, Cacciari M, Forthergill J (1997) Optimum estimators for the Weibull distribution of censored data. IEEE Trans Dielectr Electr Insul 4(4):462 – 469
20. Newland DE (1997) Practical signal analysis: Do wavelets make any difference ? In: Proceedings of 1997 ASME design engineering technical conferences, DETC′ 97. VIB-4135 September 1997
21. Paiva F, Riquelme R (2001) Wavelets and signal analysis I (In Spanish). Department of Mathematical Engineering, University of Concepción
22. Penman J, Sedding HG, Fink WT (1994) Detection and location of inter-turn short circuits in the stator windings of operating motors. IEEE Trans Energy Conv 9(4):652–658
23. Ross R (1994) Formulas to describe the bias and standard deviation of the ML-estimated Weibull shape parameter. IEEE Trans Dielectr Electr Insul 1(2):247–253
24. Ross R (1996) Bias and standard deviation due to Weibull parameter estimation for small data sets. IEEE Trans Dielectr and Electr Insul 3(1):28–42
25. Schoen R, Habetler T, Kamran F, Bartheld R (1995) Motor bearing damage detection using stator current monitoring. IEEE Trans Ind Appl 31(6):1274–1279
26. Smith JO *Mathematics of the discrete fourier transform (DFT)* . Center for Computer Research in Music and Acoustics (CCRMA), Stanford University, 2002. Web published at http://www-ccrma.stanford.edu/∼jos/mdft/
27. Sottile J, Kohler J (1993) An on line method to detect incipient failure of turn insulation in random wound motors. IEEE Trans Energy Conv 8(4):762–768

28. Stone G, Campbell S, Tetreault S (2000) Inverter-fed drives: which motor stators are at risk?. IEEE Ind Appl Mag 6(5):17–22
29. Tallam R, Habetler T, Harley R (2002) Transient model for induction machines with stator winding turn faults. IEEE Trans Ind Appl 38(3):632–637
30. The Mathworks Inc (2001) Signal processing toolbox. Matlab, The language of technical computing. Version 6.1.0.450, Release 12.1. May 2001
31. Thomson WT, Fenger M (2001) Current signature analysis to detect induction motor faults. IEEE Ind Appl Mag 7(4):26–34
32. Toliyat H, Nandi S (2002) Novel frequency-domain-based technique to detect stator inter-turn faults in induction machines using stator-induced voltages after switch-off. IEEE Trans Ind Appl 38(1):101–109
33. Williamson S, Mirzoian K (1985) Analysis of cage induction motors with stator winding faults. IEEE Trans Power Apparatus Syst PAS-104(7):1838–1842
34. Yacizi B, Kliman G (1999) An adaptive statistical time frequency method for detection of broken bars and bearing faults in motors using stator current. IEEE Trans Ind Appl 35(2):442–452